HHS Public Access

Author manuscript

Magn Reson Med. Author manuscript; available in PMC 2016 December 01.

Published in final edited form as:

Magn Reson Med. 2015 December ; 74(6): 1530–1542. doi:10.1002/mrm.25537.

In vivo longitudinal proton magnetic resonance spectroscopy on neonatal hypoxic-ischemic rat brain injury – Neuroprotective effects of acetyl-L-carnitine

Su Xu[a,b], **Jaylyn Waddell**[c], **Wenjun Zhu**[a,b], **Da Shi**[a], **Andrew D Marshall**[a,b], **Mary C McKenna**[c], and **Rao P Gullapalli**[a,b]

[a]Department of Diagnostic Radiology and Nuclear Medicine, University of Maryland School of Medicine, Baltimore, MD 21201, USA

[b]Core for Translational Research in Imaging @ Maryland, University of Maryland School of Medicine, Baltimore, MD 21201, USA

[c]Department of Pediatrics and Program in Neuroscience, University of Maryland School of Medicine, Baltimore, MD 21201, USA

Abstract

Purpose—This study evaluated the longitudinal metabolic alterations after neonatal hypoxia-ischemia (HI) in rats and tested the neuroprotective effect of acetyl-L-carnitine (ALCAR) using *in vivo* proton short-TE Point-RESolved Spectroscopy method.

Methods—Rice-Vannucci model was used on 7-day-old Sprague-Dawley rats. Data were acquired from contralateral and ipsilateral cortex and hippocampus, respectively at 4 time points (24-h, 72-h, 7-d, 28-d) post-HI. The effect of subcutaneous administration of ALCAR (100 mg/kg) immediately after HI, at 4-h, 24-h, and 48-h post-HI was determined.

Results—Significant reductions in glutathione ($p < 0.005$), *myo*-inositol ($p < 0.002$), taurine ($p < 0.001$), and total creatine ($p < 0.005$) were observed at 24-h post injury compared to the control group in the ipsilateral hippocampus of the HI rat pups. ALCAR-treated-HI rats had lower levels of lactate and maintained total creatine at 24-h and had smaller lesion size compared to the HI only rats.

Conclusion—Severe oxidative, osmotic stress, impaired phosphorylation, and a preference for anaerobic glycolysis were found in the ipsilateral hippocampus in the HI pups at 24-h post injury. ALCAR appeared to have a neuroprotective effect if administered early after HI by serving as an energy substrate and promote oxidative cerebral energy producing and minimize anaerobic glycolysis.

Keywords

neonatal hypoxic-ischemic rat brain injury; *in vivo* proton magnetic resonance spectroscopy; neuroprotection effect of acetyl-L-carnitine

Corresponding Author: Rao P Gullapalli, Department of Diagnostic Radiology and Nuclear Medicine, University of Maryland School of Medicine, 22 S. Greene Street, Baltimore, MD 21201, 410-328-2099 (phone), 410-328-5937 (fax), rgullapalli@umm.edu.

Introduction

Hypoxia ischemia (HI) is a common cause of brain injury during the perinatal period, which occurs at a rate of about 1 to 6 per 1000 near-term and term infants in the US (1). This injury can be fatal and the survivors can suffer from abnormal neurodevelopment that ranges from mild learning disabilities to profound disability including mental retardation (2–6). Neuroprotective therapies to diminish the extent of brain damage caused by HI are under active investigation (7–10). Hypothermia appears to be the most reliable intervention currently available for reducing the risk of death or disability in infants with brain injury (11, 12). The temperature reduction to 32–34 °C has now become standard care for neonatal HI brain injury (13). However, there is a strong need for additional therapies since nearly 40 percent of infants continue to have severe impairment after hypothermia (1). Recent studies have reported that a variety of pharmacological agents with antioxidant, anti-inflammatory, and anti-apoptotic actions could provide effective therapy when administered following perinatal HI (see (9) for the latest review). A key requirement for developing new therapies is to identify early non-invasive markers that are indicative of the alterations which occur early as the damage progresses and continues over hours to weeks after the initial brain insult (14). The use of animal models of neonatal HI that show injury patterns similar to those seen in human newborns can greatly facilitate the process of identifying targets to test promising therapies (15).

In vivo high resolution localized proton magnetic resonance spectroscopy (MRS) has been used as a quantitative noninvasive tool to assess the *in vivo* changes in observable cellular metabolites associated with central nervous system (CND) injury (16) and specifically it has been used to characterize the timing and pattern changes in brain metabolites after neonatal HI (17–34). Changes in brain metabolism have generally been assessed in terms of ratios of metabolites such as total choline (tCho)/ total creatine (tCr), *N*-acetylaspartate (NAA)/tCr and lactate (Lac)/NAA (18, 20, 23, 25, 28, 31). Others have reported absolute concentrations of the metabolites (21, 29, 30). For example, in the proton MRS absolute quantitation studies of a perinatal cerebral HI with severe or fatal outcomes, decreases in the concentrations of tCho and NAA and the increased concentration of Lac (21, 29) were observed.

In contrast to the clinical studies, very few studies have explored *in vivo* proton MRS on animal models. Changes in NAA and Lac following HI insult in neonatal animal brain have been reported (35–37). In a 7-day-old rat model of HI it was shown that Lac concentration in ipsilateral hemispheres was high and remained high during the first 48 h after injury (36). The same study showed that NAA concentrations ipsilateral to the occlusion decreased to 55 ± 14% during hypoxia, recovered during early post-hypoxic period and again decreased to 61 ± 25% and 41 ± 28% at 24 and 48 h post HI respectively (36). Using a clinically relevant piglet model of HI, increases in Lac/NAA, Lac/tCho and Lac/tCr were observed up to 7 d after injury (37). However, to our knowledge, there are no *in vivo* studies that have sequentially observed changes in neurometabolites following HI at the early stages and continued on for long term follow up.

Acetyl-L-carnitine (ALCAR) is an acetylated derivative of L-carnitine, a naturally occurring metabolite that facilitates transport of fatty acids across mitochondrial membranes for energy production. Carnitine and its esters prevent excess accumulation of free fatty acids in the cytoplasm and acetyl-CoA in the mitochondria, while providing sufficient acetyl-CoA for energy generation in the mitochondria (38, 39). Scafidi et al. (40) have recently demonstrated that following systemic administration, the acetyl moiety of ^{13}C-labeled ALCAR is metabolized for energy via the tricarboxylic acid (TCA) cycle in astrocytes and neurons within the forebrains of 21 to 22 d old rats. Furthermore, ^{13}C from ALCAR was incorporated into γ-aminobutyric acid (GABA), glutamate (Glu) and glutamine (Gln), which are formed subsequent to TCA cycle metabolism (40). The study demonstrated that exogenously administered ALCAR is used by the developing brain for energy metabolism. ALCAR has been shown to have neuroprotective effects by its multifactorial mode of action (41) that includes protection against oxidative stress (42, 43), augmenting the energy status (44, 45), and influencing the activity of nerve growth factor (NGF) in the nervous system by enhancing the expression of NGF receptors in the striatum and hippocampus of rats during development (46). Carnitine levels can be low in infants (47) and administration of high levels of carnitine prior to injury was shown to be neuroprotective in the rat model of neonatal HI injury (48). Treatment with ALCAR after traumatic brain injury in immature rats significantly improved behavioral outcome and decreased lesion size (40, 49).

The present *in vivo* study aimed at evaluating the regional brain metabolism alterations in survivors of cerebral HI (induced aged 7 d) rats at 24 h, 72 h, 7 d, and 28 d following injury. Given the potential benefits of ALCAR, we also evaluated the effects of post-insult ALCAR treatment on the HI rats.

Methods

Animal procedure

A modified version of the Rice-Vannucci model (50) of HI was used to induce HI brain injury in Sprague-Dawley rats at postnatal day (PND) 7. Within 24 h of birth, litters were culled to 9 pups. All pups included in the study appeared healthy with milk bands at 24 h after birth. Litters were balanced by sex when possible (5:4) and weighed between 12.5–15.5 g on the day of HI. Pups in this weight range were randomly assigned to one of three conditions: 1) untreated control group (Control, 6 male and 6 female) 2) HI (6 male and 6 female) 3) HI+ALCAR (6 male and 6 female). Pups subjected to HI were anesthetized with isoflurane (3% for 1 min, maintained with 1.5%) and the right internal carotid artery was ligated in two places and severed. The average surgery time was 4.5 min. After surgery, all pups were maintained in a water bath at 37°C for 30 min to ensure body temperature does not drop while pups recover from anesthesia. Pups were then returned to the dam in a clean home cage for 1 h. During this time, the home cage was warmed from underneath using deltaphase isothermal pads (37°C) to prevent cooling of pups. Hypoxia was conducted in pre-warmed 450 ml glass jars (2 pups per jar) in a 37°C water bath as described in the Rice-Vannucci method (50). Jars were sealed, flushed with warmed and humidified gas mix of 8% oxygen in nitrogen at 1 L/min and placed in the 37°C water bath for 75 min. After hypoxia the pups recovered at 37°C in room air for 2 h prior to return to the dam. Control

pups were removed from the dam and warmed at the same intervals as pups subjected to HI. Acetyl-L-carnitine hydrochloride (Sigma-Aldrich Corporation, St Louis, MO, USA) was freshly diluted into 8.2 % sodium bicarbonate and the pH was confirmed to be 7–7.4 prior to administration. The HI+ALCAR pups were injected subcutaneously with 4 doses of ALCAR (100 mg/kg) immediately after HI, at 4 h, 24 h, and 48 h after HI. Saline was injected at the same time points to the HI and control groups. All animal procedures were approved by the Institutional Animal Care and Use Committee at the University of Maryland School of Medicine.

In vivo proton MRS experiments

In vivo proton MRS experiments were performed on a Bruker BioSpec 70/30USR Avance III 7T horizontal bore MR scanner (Bruker Biospin MRI GmbH, Germany) equipped with a BGA12S gradient system and interfaced to a Bruker Paravision 5.1 console. A Bruker four-element proton surface coil array was used as the receiver and a Bruker 72-mm linear-volume coil as the transmitter. The rat was anesthetized in an animal chamber using medical air (1 L/min) and isoflurane (2.5 – 3 %). The animal was then placed prone in an animal holder and the four-element proton surface coil array was positioned and fixed over the head of the animal. The animal holder was moved to the center of the magnet and the isoflurane level was changed to 2 %. The level of isoflurane was further adjusted based on changes in the respiration rate of each animal for the remainder of the experiment. A MR compatible small animal monitoring and gating system (SA Instruments, Inc., New York, USA) was used to monitor the animal respiration rate and body temperature. The animal body temperature was maintained at 36–37°C using warm water circulation and a cotton blanket on the back of the animal.

A three-slice (axial, mid-sagittal, and coronal) scout image using fast low angle shot (FLASH) sequence (51, 52) was obtained to center the rat's brain in the imaging field of view. A fast shimming procedure (FASTMAP) was used to improve the B_0 homogeneity in the region of interest (53). Both proton density- and T_2-weighted images were obtained for anatomic reference using a two-dimensional rapid acquisition with relaxation enhancement (RARE) sequence covering the entire brain in the coronal plane (repetition time (TR) / echo time (TE) $_{eff1}$/ TE $_{eff2}$ = 5500/18.9/56.8 ms, RARE factor = 4, field of view = 25 × 25 mm^2, slice thickness = 0.5 mm, in-plane resolution = 100 × 100 μm^2, number of averages (NA) = 2, number of slices = 20).

For proton MRS, adjustments of all first- and second-order shims over the voxel of interest were accomplished with the FASTMAP procedure. A custom modified short-echo-time PRESS (Point-RESolved Spectroscopy) pulse sequence (TR/TE = 2500/10 ms, NA = 300) (54) was used for MRS data acquisition from four fixed regions regardless of whether lesion was detected by MRI or not including the left and right cortex (1.5 (ventral – dorsal) × 3.5 (left – right) × 3.0 (anterior – posterior) mm^3), left and right hippocampus (2.0 (ventral – dorsal) × 3.5 (left – right) × 2.5 (anterior – posterior) mm^3) (Fig. 1). The voxel location and size was decided on PND 8 during the experiment when the brain size was the smallest. Care was taken to incorporate most of the hippocampus into the voxel and minimize any extra-hippocampal tissue. The contamination of tissue from other regions of the brain was

further minimized at PND 10, 14 and 35 d. Visual inspection of the voxel at PND 8 shows less than 10 % contamination from extra hippocampal tissue and much less during latter days. The acquisition time for each voxel was 12 min. The unsuppressed water signal from each of the prescribed voxels was obtained to serve as a reference for determining the specific metabolite concentrations. Each rat pup was scanned at 4 time points after the end of the HI procedure: 24 h, 72 h, 7 d, and 28 d. Thus, the age of the pups at the time of the scans corresponded to 8 (PND 8), 10 (PND 10), 14 (PND 14) and 35 (PND 35) days, respectively. Among all the rat pups, one HI female rat and one HI+ALCAR male rat died during the last MRS acquisition on day 28 following injury. MRS data on the ipsilateral hippocampus from these two rats could not be obtained. In addition, two pups from the control group died during the 72 h spectrum acquisition and were replaced by two other peers.

Data analysis and statistics

Quantification of the MRS was based on frequency domain analysis using "Linear Combination of Model spectra" (LCModel) (55). A simulated basis set of model metabolites appropriate for our acquisition parameters was obtained from Stephen Provencher (LCMODEL Inc., Oakville, ON, Canada) (personal communication). Absolute concentrations were estimated with the LCModel automatic procedure which includes the relaxation corrections in the model spectra (56). All concentrations were expressed as mean ± standard error of the mean (SE). Only those metabolites that passed the Cramer-Rao lower bound of 25% in more than 90 % of the spectra were considered for further analysis. Our choice of this threshold was based on previous studies that considered this as an acceptable threshold for reliably quantifying metabolites when studying the developing rat brain. (57, 58). Statistical analyses were performed for each region of the brain for the three groups at each time point using a two-way repeated analysis of variance (ANOVA) with one factor, repetition, followed by *post hoc* Tukey's test for multiple comparison corrections. Significance level was set at $P<0.05$. The following neurochemicals were observed: creatine (Cr), GABA, glucose (Glc), Gln, Glu, glycerophosphocholine (GPC), glutathione (GSH), *myo*-inositol (Ins), Lac, NAA, *N*-acetylaspartylglutamate (NAAG), phosphocholine (PCh), phosphocreatine (PCr), taurine (Tau), tCr = Cr+ PCr, tCho = GPC + PCh, and glutamate/glutamine complex (Glx =Glu +Gln).

Results

Lesion Characteristics on T_2-Weighted MRI

Structural T_2-weighted images revealed hyperintensity lesions ipsilateral (Fig. 2) on 8 out of 12 HI only pups and 7 out 12 HI+ALCAR pups at 24 h post injury (PND 8). The edema was accompanied with structural deformations in most animals. In some animals in HI only group the lesion extended to the surface of the contralateral cortex (Fig. 2a). The extent of edema and structural deformation was much smaller in HI+ALCAR group (Fig. 2b). By 72 h, edema was clearly visible in the HI rats. Diffuse hyperintensity in the ipsilateral cortex and hippocampus, and tissue swelling accompanied by a midline shift toward the contralateral hemisphere was observed in HI rat pups (Fig. 2a). At 72 h the severity of injury was much less in HI+ALCAR group (Fig. 2b). Ipsilateral tissue swelling subsided by 7 d,

however, giving way to cortical thinning in HI group. Very little structural deformations were observed at 7 d in the HI+ALCAR rat pups. By 28 d, cysts with discrete boundaries were clearly visible in both ipsilateral cortex and hippocampus in the HI group, whereas the brains of the HI+ALCAR animals were largely normal.

Normal Developmental Changes

Significant differences in temporal changes were observed from the two-way repeated measures ANOVA analysis over the 28 d of observation (PND 8 to PND 35) for all metabolites except for tCr in the ipsilateral hippocampus in all the three animal groups. Tab. 3 and 4 provide the statistical significances from the two-way ANOVA analysis for various metabolites from the hippocampus and the cortex, respectively. Trajectories of developmental changes for metabolites from the ipsilateral hippocampus and the ipsilateral cortex are shown in Fig. 3. Relatively similar developmental patterns were observed in the hippocampus and cortex for each of the metabolites; however there were subtle differences in the trajectory in cortex and hippocampus for some metabolites (e.g. NAA concentration increased more rapidly from PND 10 to PND 35 in cortex than in hippocampus,; Tau concentration decreased more rapidly for PND 8 to PND 10 in cortex than in hippocampus). The direction of change with age differed among metabolites studied. The concentration of GABA, Gln, Glu, and NAA increased with age from PND 8 to PND 35 (Fig. 3a, c). In contrast, the concentration of a number of metabolites decreased or remained constant from PND 8 to PND 35. Tau concentration decreased more than 3 fold from PND 8 to PND 35 d of age. (Fig. 3b, d). A dramatic reduction in GSH was observed at PND 10, and then the concentration stabilized at PND 14 to PND 35 (Fig. 3b, d). Ins and tCr concentrations in both the ipsilateral cortex and hippocampus decreased from PND 8 to PND 14, followed by an increase in concentration between PND 14 and PND 35 d (Fig. 3b, d). The tCho concentration in both the ipsilateral cortex and hippocampus remained relatively constant between PND 8 and PND 35 (Fig. 3b, d). There were no statistical significances in metabolites between the ipsilateral and contralateral cortex in control rats. However, the NAA level in control rats was significantly higher in the ipsilateral hippocampus ($F [1, 33] = 71.12$, $p < 0.001$) compared to its contralateral side at PND 8 ($p < 0.001$), PND 10 ($p < 0.001$), PND 14 ($p < 0.05$), and PND 35 ($p < 0.001$). NAA+NAAG showed a similar trend as NAA.

Metabolic changes in hippocampus and cortex following HI

Representative *in vivo* high resolution ^{1}H MRS from the ipsilateral hippocampus from one HI rat at 24 h post injury or PND 8 (Fig. 4a), 72 h post injury or PND 10 (Fig. 4b), 7 d post injury or PND 14 (Fig. 4c), and 28 d post injury or PND 35 (Fig. 4d) are shown in Fig. 4. Most of the neurometabolites are clearly discernible. Among them, GABA, Gln, Glu, Ins, NAA, Tau, GSH, tCho, NAA+NAAG, tCr, and Glx typically passed the set CRLB threshold criteria. The concentrations of the metabolites in the ipsilateral and contralateral hippocampus (Tab. 1), and the ipsilateral and the contralateral cortex (Tab. 2) are summarized for each animal group at each time point after HI.

The most profound changes in metabolites after HI injury were detected in the ipsilateral hippocampus as shown in Tab. 3 and Fig. 5. Two-way repeated measures ANOVA revealed

significant interactions between group and time for a number of metabolites including GSH ($F [6, 97] = 5.730$, $p < 0.001$), Ins ($F [6, 97] = 5.174$, $p < 0.001$), Tau ($F [6, 97] = 6.358$, $p < 0.001$), and tCr ($F [6, 97] = 4.206$, $p < 0.001$) (Tab. 3 and Fig. 5). *Post hoc* Tukey's test revealed significant changes in GSH ($p < 0.005$), Ins ($p < 0.002$), Tau ($p < 0.001$), and tCr ($p < 0.005$) between the control and HI rat pups at 24 h following injury for these metabolites after correcting for multiple comparisons. Although, Tau ($p < 0.001$), GSH ($p < 0.058$), and Ins ($p < 0.055$) levels were either significantly lower or demonstrated a trend to lower values in HI+ALCAR rat pups compared to control animals, tCr was not statistically different between control and HI+ALCAR rat pups which may reflect the protective effects of ALCAR. There were no statistically significant interactions between groups and time after HI in the ipsilateral cortex, contralateral hippocampus, and contralateral cortex (Tab. 3 and 4).

While reliable, the Vannucci model can lead to variability in the severity of injury (51). This may explain why detectable levels of Lac were not found in all animals. Data density plots of the level of Lac in the ipsilateral and contralateral regions of the hippocampus are shown in Fig. 6. When generating these plots a value of zero was assigned when LCModel was unable to quantify the metabolite. At 24 h after HI injury, 9 out of 12 HI animals had higher levels of Lac compared to the mean Lac level of the 12 control animals. In contrast, only 4 out of 12 animals in HI+ALCAR group presented with Lac levels that were higher than that of the control group in the ipsilateral hippocampus. The high level of Lac combined with the tCr depletion in the HI rats clearly indicates impaired oxidative phosphorylation and a corresponding reliance on anaerobic glycolysis for energy generation within the ipsilateral hippocampus following HI injury. In addition, tCr levels remained relatively high (Fig. 5d) in the ipsilateral hippocampus in the ALCAR treated animals at 24 hour after HI injury, suggesting a possible protective effect on oxidative phosphorylation in the mitochondria. Increased glucose was observed in the MR spectra in the ipsilateral side of brain of some HI rats after injury; however, analysis of the Glc levels did not reveal any consistent differences under any conditions in this study.

Discussion

To our knowledge, this is the first study to characterize the longitudinal changes of neurometabolites *in vivo* in the developing hippocampus and the cortex of neonatal HI rats. In this study we observed the alteration of metabolic profiles in the hippocampus and the cortex over 28 d during the critical developmental period on a 7-days-old rat model of neonatal HI. The main alterations in metabolite concentration after HI occurred in the ipsilateral hippocampus of the HI rats where significant reductions in GSH, Ins, Tau, and tCr were observed at 24 h after HI. An imbalance in these metabolites during this important period of synaptogenesis and very early myelination has implications for important functions such as osmoregulation, oxidative stress, signal transduction, and neuromodulation that could have a profound impact on brain development. Our study also indicates that part of this disruption could be mitigated by treatment with ALCAR which may have a neuroprotective role through the maintenance of tCr and reduced levels of Lac thus stabilizing the neurometabolic profile in the ipsilateral hippocampus where the largest effect was observed in the HI+ALCAR rats at 24 h.

Neurometabolic Profile of Developing Brain

This study largely corroborates previously published results regarding neurometabolites in the rat cortex and the hippocampus except for Ins. Tkác et al. (59) reported significant increases in Ins from PND 7 to PND 28 in both mid cortex and right hippocampus. While our results are largely in agreement over the 28 d of observation, we did find a decrease in Ins concentrations up to PND14 followed by an increase by PND35 in both the cortex and the hippocampus, It should be noted that the present study used room air with isoflurane for anesthesia to avoid further damage from hyperoxia; whereas, Tkac et al. (59) used isoflurane with equal parts of N_2:O_2 for anesthesia induction.

It is noted that NAA levels were distributed asymmetrically in the right and left hippocampus. NAA concentration was higher in the right hippocampus compared to its left side in the normal brain from PND 8 to PND 35. Brain asymmetry has been observed in animals and humans in terms of structure, function and behavior (60). Early studies of asymmetry in the cross-sectional width of the hippocampus reported that the right hippocampus was significantly thicker than the left hippocampus in the neonatal male rats by about 8% at PND 6 to PND 26 (61); the difference decreased with age (from PND 6 to PND 896) until the asymmetry was no longer statistically significant (at PND 90) (62). During early postnatal CNS development, NAA is an important source of acetyl moieties used for synthesis of myelin lipids in brain (63). Therefore, a right greater than left NAA asymmetry in the hippocampus may reflect a right greater than left neuronal growth during the period PND 8 to PND 35 and also was supported by a thicker right hippocampus found in previous studies (61, 62). It should be noted that NAA asymmetry may only exist during these transitional developmental stage (62).

Oxidative stress

The neonatal brain, with its high concentrations of unsaturated fatty acids, high rate of oxygen consumption, low concentrations of antioxidants, and presence of redox-active iron, is particularly vulnerable to oxidative damage (64). In the very immature brain, oligodendrocyte progenitor cells and preoligodendrocytes are selectively vulnerable to the depletion of antioxidants or exposure to exogenous free radicals (65). Mature oligodendrocytes, in contrast, are highly resistant to oxidative stress, owing in part to differences in the levels of expression of antioxidant enzymes and proteins involved in programmed cell death (65). Oxidative stress was hypothesized as the first response to the neonatal brain injury (66).

GSH is an important antioxidant for protecting cells from oxidative stress (67). The brain consumes a large quantity of oxygen, making it particularly susceptible to oxidative stress (68). Natural formation of oxidants during mitochondrial electron transport, auto-oxidation of some neurotransmitters (e.g. norepinephrine, dopamine), and initiation of events during hypoxia or ischemia can result in oxidant formation and subsequent tissue damage (69). Brain ischemia initiates a complex cascade of metabolic events, several of which involve the generation of nitrogen and oxygen free radicals (70). These free radicals and related reactive chemical species mediate much of the damage that occurs after transient brain ischemia, and in the penumbral region of infarcts caused by permanent ischemia (70). GSH deficiency

induced in newborn rats by application of an inhibitor of γ-glutamylcysteine synthetase, buthionine sulfoximine (BSO), leads to mitochondrial damage in brain (71). Furthermore, reduction of the brain GSH content by BSO enhances the toxic effects of insults that are associated with elevated production of reactive oxygen species, i.e., ischemia (72). The dramatic depletion of GSH in this study suggests a severe oxidative stress in ipsilateral hippocampus at 24 h after HI.

Tau is a ubiquitous sulfur-containing amino acid that has been proposed to be an antioxidant (73). It is present in high concentration in the immature brain and this concentration decreases with age (74, 75). Tau and GSH synthesis are tightly coupled, sharing the same precursor, cysteine (76, 77). Thus the decrease in both GSH and Tau at 24 h after HI may reflect a decrease in precursor cysteine levels. Tau depletion in ipsilateral hippocampus at 24 h after HI found in this study could contribute to oxidative stress in the damaged hippocampus since Tau has been shown to be protective against glutamate-induced excitotoxicity through several identified mechanisms including interactions with Ca^{2+} or Cl^{-} channels (78 – 81), and the *N*-Methyl-D-aspartate receptor (82).

Osmotic Stress

Brain edema was reported in HI PND 7 rats with high tissue water content in the ipsilateral cerebral hemisphere (89.7 % in HI vs. 87.7 % in control at 24 h post HI) (83) indicating osmotic stress. Astrocytes have been shown to rapidly swell in response to oxygen/glucose deprivation *in vitro* and to cardiac arrest *in vivo* revealed by two-photon microscopy (84). Tau (85–87) and Ins (88) are two of the major osmolytes present in the brain and are consider to be glial cell markers (89, 90). Extracellular Tau has been shown to increase in response to hypoosmotic swelling (91). Ins levels increased in the rodent brains during chronically hypernatremia (88, 92) and decreased in hyponatremia (92). Reduction of Tau and Ins at 24 h within the ipsilateral hippocampus suggests loss of water homeostasis and alterations in glial osmolytes following HI.

Impaired Energy Generation

Lac levels are higher in the neonatal brain compared to a mature rat brain and the signal is detectable using MRS (93). Lac is utilized as an energy substrate in developing brain (68, 94). Seventy percent of the cerebral metabolic requirements are met by Lac in the immediate postnatal period and ketone bodies are important during the suckling period (68). At weaning glucose becomes the major energy source for brain (68, 93). Lac level was reported elevated in neonatal HI rats by *in vivo* proton MRS (35, 36) which is in agreement with our study. The elevated Lac in neonatal HI brains is likely related to greater anaerobic glycolysis for energy generation and less oxidative energy metabolism compared to the controls.

The Cr-PCr system is essential for the maintenance of cellular adenosine triphosphate, serving as a spatial and temporal energy buffer in cells with fluctuating energy demand (95). Synthesized in the liver and transported to the brain, Cr, according to *in vitro* studies, is 2 to 4-fold more concentrated in glial cells than in neurons (96), with quite large regional variations, and with higher levels in gray than in white matter. Previous MRS studies have shown that Cr increases in human infants before and around term and also increases over the

first 2 years of age (97). In spiny mouse, a precocial rodent that matches the human perinatal development, the Cr content of the placenta and fetal brain increases from midgestation to term, and continues to increase in the second postnatal week in the brain (98). In the current study, the total level of Cr and PCr was reduced in the ipsilateral hippocampus at 24 h after HI injury compared to control animals, which may be indicative of impaired oxidative phosphorylation in the region. Taken together, the reduced levels of tCr and elevated Lac are suggestive of impaired energy balance in the ipsilateral hippocampus.

Neuroprotective Effects of ALCAR

HI rats treated with ALCAR maintained relatively high tCr and low Lac levels in the ipsilateral hippocampus compared to HI rats at 24 h post injury. These effects of ALCAR on levels of cerebral energy metabolites are consistent with the hypothesis that the acetyl component of ALCAR is metabolized in the brain, thereby promoting oxidative cerebral energy production and minimizing anaerobic glycolysis and lactic acidosis.

Many animal studies and clinical reports demonstrate neuroprotection of brain from injury by ALCAR. ALCAR has several proposed modes of action including acting as an energy substrate (99), preventing inflammation, compensating for impaired pyruvate dehydrogenase complex (PDHC) activity, and the ability to activate the Nrf2/antioxidant response element (ARE) pathway of anti-oxidant and anti-inflammatory gene expression (100). Post ischemic administration of ALCAR improved neurological outcome following global cerebral ischemia in a clinically relevant model of adult canine cardiac arrest (101). The improved outcome after global ischemia was associated with reduced brain Lac levels at 2 to 24 h of reperfusion, consistent with the hypothesis that ALCAR stimulates post ischemic cerebral aerobic energy metabolism and reduces tissue lactic acidosis caused by accelerated anaerobic glycolysis (101). ALCAR treatment has also been shown to reduce post ischemic oxidative damage to proteins (42), protects against loss of PDHC in adult brain (43), and suppressed systemic elevation of inflammatory cytokines (102). In the context of the overwhelming evidence from these earlier studies it is not surprising to find that GSH and Ins levels remain close to the control levels on the ALCAR treated animals following HI injury in the present study, consistent with the concept that ALCAR may be neuroprotective following HI injury.

In summary, this high resolution *in vivo* localized proton MRS study clearly demonstrated significant increases in oxidative and osmotic stress, impaired phosphorylation, and a preference for anaerobic glycolysis at 24 h following HI in the hippocampus. The results indicate that ALCAR provides neuroprotection if administered early after injury by serving as an energy substrate and promote oxidative cerebral energy producing and minimize anaerobic glycolysis.

Acknowledgments

This study was supported by NIH grant to Mary C. McKenna (5P01 HD016596).

References

1. Shankaran S. Neonatal encephalopathy: treatment with hypothermia. J Neurotrauma. 2009; 26:437–443. [PubMed: 19281415]
2. Robertson CM, Finer NN, Grace MG. School performance of survivors of neonatal encephalopathy associated with birth asphyxia at term. J Pediatr. 1989; 114:753–760. [PubMed: 2469789]
3. Vannucci RC, Perlman JM. Interventions for perinatal hypoxic-ischemic encephalopathy. Pediatrics. 1997; 100:1004–1014. [PubMed: 9374573]
4. Badawi N, Felix JF, Kurinczuk JJ, Dixon G, Watson L, Keogh JM, Valentine J, Stanley FJ. Cerebral palsy following term newborn encephalopathy: a population-based study. Dev Med Child Neurol. 2005; 47:293–298. [PubMed: 15892370]
5. Ambalavanan N, Carlo WA, Shankaran S, Bann CM, Emrich SL, Higgins RD, Higgins RD, Tyson JE, O'Shea TM, Laptook AR, Ehrenkranz RA, Donovan EF, Walsh MC, Goldberg RN, Das A. Predicting outcomes of neonates diagnosed with hypoxemic-ischemic encephalopathy. Pediatrics. 2006; 118:2084–2093. [PubMed: 17079582]
6. Perlman M, Shah PS. Hypoxic-ischemic encephalopathy: challenges in outcome and prediction. J Pediatr. 2011; 158(2 Suppl):e51–54. [PubMed: 21238707]
7. Vannucci RC. Current and potentially new management strategies for perinatal hypoxic-ischemic encephalopathy. Pediatrics. 1990; 85:961–968. [PubMed: 2160066]
8. Whitelaw A. Systematic review of therapy after hypoxic-ischaemic brain injury in the perinatal period. Semin Neonatol. 2000; 5:33–40. [PubMed: 10802748]
9. Goñi-de-Cerio F, Lara-Celador I, Alvarez A, Hilario E. Neuroprotective therapies after perinatal hypoxic-ischemic brain injury. Brain Sci. 2013; 3:191–214. [PubMed: 24961314]
10. Chicha L, Smith T, Guzman R. Stem cells for brain repair in neonatal hypoxia-ischemia. Child Nerv Syst. 2014; 30:37–46.
11. Compagnoni G, Pogliani L, Lista G, Castoldi F, Fontana P, Mosca F. Hypothermia reduces neurological damage in asphyxiated newborn infants. Biol Neonate. 2002; 82:222–227. [PubMed: 12381928]
12. Thoresen M, Whitelaw A. Therapeutic hypothermia for hypoxic-ischaemic encephalopathy in the newborn infant. Curr Opin Neurol. 2005; 18:111–116. [PubMed: 15791139]
13. Shah PS, Ohlsson A, Perlman M. Hypothermia to treat neonatal hypoxic ischemic encephalopathy: A systemic review. Arch Pediatr Adolesc Med. 2007; 161:951–958. [PubMed: 17909138]
14. Robertson CL. Mitochondrial dysfunction contributes to cell death following traumatic brain injury in adult and immature animals. J Bioenerg Biomembr. 2004; 36:363–368. [PubMed: 15377873]
15. Vannucci RC, Connor JR, Mauger DT, Paimer C, Smith MB, Towfighi J, Vannucci SJ. Rat model of perinatal hypoxic-ischemic brain damage. J Neurosci Res. 1999; 55:158–163. [PubMed: 9972818]
16. Xu S, Chuo J, Shi D, Roys S, Fiskum G, Gullapalli R. Early Microstructural and Metabolic Changes Following Controlled Cortical Impact Injury in rat: A Magnetic Resonance Imaging and Spectroscopy Study. J Neurotrauma. 2011; 28:2091–2102. [PubMed: 21761962]
17. Dubowitz LM, Bydder GM. Nuclear magnetic resonance imaging in the diagnosis and follow-up of neonatal cerebral injury. Clin Perinatol. 1985; 12:243–260. [PubMed: 3978988]
18. Peden CJ, Rutherford MA, Sargentoni J, Cox IJ, Bryant DJ, Dubowitz LMS. Proton spectroscopy of the neonatal brain following hypoxic-ischaemic injury. Dev Med Child Neurol. 1993; 35:502–510. [PubMed: 8504892]
19. Hanrahan JD, Sargentoni J, Azzopardi D, Manji K, Cowan FM, Rutherford MA, Cox IJ, Bell JD, Bryant DJ, Edward AD. Cerebral metabolism within 18 h of birth asphyxia: a proton magnetic resonance spectroscopy study. Pediatr Res. 1996; 39:584–590. [PubMed: 8848329]
20. Penrice J, Cady EB, Lorek A, Wylezinska M, Amess PN, Aldridge RF, Stewart AL, Wyatt JS, Reynold EOR. Proton magnetic resonance spectroscopy of the brain in normal preterm and term infants, and early changes following perinatal hypoxiaischaemia. Pediatr Res. 1996; 40:6–14. [PubMed: 8798238]

21. Cady EB. Metabolite concentrations and relaxation in perinatal cerebral hypoxic-ischaemic injury. Neurochem Res. 1996; 21:1043–1052. [PubMed: 8897467]
22. Cady EB. Magnetic resonance spectroscopy in neonatal hypoxic-ischaemic insults. Child Nerv Syst. 2001; 17:145–149.
23. Holshouser SA, Ashwal S, Luh GY, Shu S, Kahlon S, Auld KL, Tomasi LG, Perkin RM, Hinshaw DB Jr. Proton spectroscopy after acute central nervous system injury; outcome prediction in neonates, infants, and children. Radiology. 1997; 202:487–496. [PubMed: 9015079]
24. Barkovich AJ, Baranski K, Vigneron D, Partridge JC, Hallam DK, Hajnal BL, Ferriero DM. Proton MR spectroscopy for the evaluation of brain injury in asphyxiated, term neonates. AJNR Am J Neuroradiol. 1999; 20:1399–1405. [PubMed: 10512219]
25. Amess PN, Penrice J, Wylezinska M, Lorek A, Townsend J, Wyatt JS, Amiel-Tison C, Cady EB, Stewart A. Early brain proton magnetic resonance spectroscopy and neonatal neurology related to neurodevelopmental outcome at 1 year in term infants after presumed hypoxic-ischaemic brain injury. Dev Med Child Neurol. 1999; 41:436–445. [PubMed: 10454226]
26. Robertson NJ, Lewis RH, Cowan FM, Allsop JM, Counsell SJ, Edward AD, Cox IJ. Early increases in brain myo-inosotol measured by proton magnetic resonance spectroscopy in term infants with neonatal encephalopathy. Pediatr Res. 2001; 50:692–700. [PubMed: 11726726]
27. Groenendaal F, Roelants-van Rijn AM, van der Grond J, Toet MC, de Vries LS. Glutamate in cerebral tissue of asphyxiated neonates during the first week of life demonstrated in vivo using proton magnetic resonance spectroscopy. Biol Neonate. 2001; 79:254–257. [PubMed: 11275661]
28. Fan G, Wu Z, Chen L, Guo Q, Ye B, Mao J. Hypoxic-ischemic encephalopathy in full-term neonate: correlation of proton MR spectroscopy with MR imaging. Eur J Radiol. 2003; 45:91–98. [PubMed: 12536086]
29. Cheong JL, Cady EB, Penrice J, Wyatt JS, Cox IJ, Robertson NJ. Proton MR spectroscopy in neonates with perinatal cerebral hypoxic-ischemic injury: metabolite peak-area ratios, relaxation times, and absolute concentrations. AJNR Am J Neuroradiol. 2006; 27:1546–1554. [PubMed: 16908578]
30. Boichot C, Walker PM, Durand C, Grimaldi M, Chapuis S, Gouyon JB, Brunotte F. Term neonate prognoses after perinatal asphyxia: contributions of MR imaging, MR spectroscopy, relaxation times, and apparent diffusion coefficients. Radiology. 2006; 239:839–848. [PubMed: 16641336]
31. Shanmugalingam S, Thornton JS, Iwata O, Priest AN, Ordidge RJ, Cady EB, Wyatt JS, Robertson NJ. Comparative prognostic utilities of early quantitative magnetic resonance imaging spin-spin relaxometry and proton magnetic resonance spectroscopy in neonatal encephalopathy. Pediatrics. 2006; 118:1467–1477. [PubMed: 17015537]
32. Zhu W, Zhong W, Qi J, Yin P, Wang C, Chang L. Proton magnetic resonance spectroscopy in neonates with hypoxicischemic injury and its prognostic value. Transl Res. 2008; 152:225–232. [PubMed: 19010293]
33. Thayyil S, Chandrasakaran M, Taylor A, Bainbridge A, Cady EB, Chong WK, Murad S, Omar RZ, Robertson NJ. Cerebral magnetic resonance biomarkers in neonatal encephalopathy: a meta-analysis. Pediatrics. 2010; 125:e382–e395. [PubMed: 20083516]
34. van Doormaal PJ, Meiners LC, ter Horst HJ, van der Veere CN, Sijens PE. The prognostic value of multivoxel magnetic resonance spectroscopy determined metabolite levels in white and grey matter brain tissue for adverse outcome in term newborns following perinatal asphyxia. Eur Radiol. 2011; 22:772–778. [PubMed: 22057247]
35. Behar KL, den Hollander JA, Stromski ME, Ogino T, Shulman RG, Petroff OA, Prichard JW. High-resolution ^{1}H nuclear magnetic resonance study of cerebral hypoxia in vivo. Proc Natl Acad Sci U S A. 1983; 80:4945–4948. [PubMed: 6576367]
36. Malisza KL, Kozlowski P, Ning G, Bascaramurty S, Tuor UI. Metabolite changes in neonatal rat brain during and after cerebral hypoxia-ischemia: a magnetic resonance spectroscopic imaging study. NMR Biomed. 1999; 12:31–38. [PubMed: 10195327]
37. Vial F, Serriere S, Barantin L, Montharu J, Nadal-Desbarats L, Pourcelot L, Seguin F. A newborn piglet study of moderate hypoxic-ischemic brain injury by ^{1}H-MRS and MRI. Magn Reson Imaging. 2004; 22:457–465. [PubMed: 15120164]

38. Arenas J, Rubio JC, Martin MA, Campos Y. Biological roles of L-carnitine in perinatal metabolism. Early Hum Dev. 1998; 53:S43–S50. [PubMed: 10102654]
39. Onofrj M, Ciccocioppo F, Varanese S, di Muzio A, Calvani M, Chiechio S, Osio M, Thomas A. Acetyl-L-carnitine: from a biological curiosity to a drug for the peripheral nervous system and beyond. Expert Rev Neurother. 2013; 13:925–936. [PubMed: 23965166]
40. Scafidi S, Fiskum G, Lindauer SL, Bamford P, Shi D, Hopkins I, McKenna MC. Metabolism of acetyl-L-carnitine for energy and neurotransmitter synthesis in the immature rat brain. J Neurochem. 2010a; 114:820–831. [PubMed: 20477950]
41. Zanelli SA, Solenski NJ, Rosenthal RE, Fiskum G. Mechanisms of ischemic neuroprotection by acetyl-L-carnitine. Ann N Y Acad Sci. 2005; 1053:153–161. [PubMed: 16179519]
42. Liu Y, Rosenthal RE, Starke-Reed P, Fiskum G. Inhibition of post–cardiac arrest brain protein oxidation by acetyl-L-carnitine. Free Rad Biol Med. 1993; 15:667–670. [PubMed: 8138193]
43. Bogaert YE, Rosenthal RE, Fiskum G. Post-ischemic inhibition of cerebralcortex pyruvate dehydrogenase. Free Rad Biol Med. 1994; 6:811–820. [PubMed: 8070685]
44. Colucci WJ, Gandour RD. Carnitine acyltransferase: a review of its biology, enzymology and bioorganic chemistry. Bioorg Chem. 1988; 16:307–334.
45. Bremer J. The role of carnitine in intracellular metabolism. J Clin Chem Clin Biochem. 1990; 28:297–301. [PubMed: 2199593]
46. Chiechio S, Copani A, De Petris L, Morales ME, Nicoletti F, Gereau RW 4th. Transcriptional regulation of metabotropic glutamate receptor 2/3 expression by the NF-kappaB pathway in primary dorsal root ganglia neurons: a possible mechanism for the analgesic effect of l-acetylcarnitine. Mol Pain. 200610.1186/1744-8069-2-20
47. Coran AG, Drongowski RA, Baker PJ. The metabolic effects of oral L-carnitine administration in infants receiving total parenteral nutrition with fat. J Pediatr Surg. 1985; 20:758–764. [PubMed: 3936908]
48. Wainwright MS, Mannix MK, Brown J, Stumpf DA. L-carnitine reduces brain injury after hypoxia-ischemia in newborn rats. Pediatr Res. 2003; 54:688–695. [PubMed: 12904603]
49. Scafidi S, Racz J, Hazelton J, McKenna MC, Fiskum G. Neuroprotection by acetyl-L-carnitine after traumatic injury to the immature rat brain. Dev Neurosci. 2010b; 32:480–487. [PubMed: 21228558]
50. Rice JE III, Vannucci RC, Brierley JB. The influence of immaturity on hypoxic-ischemic brain damage in the rat. Ann Neurol. 1981; 9:131–141. [PubMed: 7235629]
51. Frahm J, Haase A, Matthaei D. Rapid NMR imaging of dynamic processes using the FLASH technique. Magn Reson Med. 1996; 3:321–327. [PubMed: 3713496]
52. Haase A, Frahm J, Matthaei D, Hänicke W, Merboldt KD. FLASH imaging: rapid NMR imaging using low flip angle pulses. J Magn Res. 1986; 67:258–266.
53. Gruetter R. Automatic, localized in vivo adjustment of the first- and second-order shim coils. Magn Reson Med. 1993; 29:804–811. [PubMed: 8350724]
54. Xu S, Ji Y, Chen X, Yang Y, Gullapalli RP, Masri R. *In vivo* high-resolution localized ^{1}H MR spectroscopy in the awake rat brain at 7 T. Magn Reson Med. 2012; 69:937–943. [PubMed: 22570299]
55. Provencher SW. Estimation of metabolite concentrations from localized *in vivo* proton NMR spectra. Magn Reson Med. 1993; 30:672–679. [PubMed: 8139448]
56. Provencher SW. Automatic quantitation of localized in vivo ^{1}H spectra with LCModel. NMR Biomed. 2001; 14:260–264. [PubMed: 11410943]
57. Morgan JJ, Kleven GA, Tulbert CD, Olson J, Horita DA, Ronca AE. Longitudinal ^{1}H MRS of rat forebrain from infancy to adulthood reveals adolescence as a distinctive phase of neurometabolite development. NMR Biomed. 2013; 26:683–691. [PubMed: 23322706]
58. Harris JL, Yeh HW, Choi IY, Lee P, Berman NE, Swerdlow RH, Craciunas SC, Brooks WM. Altered neurochemical profile after traumatic brain injury: (1)H-MRS biomarkers of pathological mechanisms. J Cereb Blood Flow Metab. 2012; 32:2122–2134. [PubMed: 22892723]
59. Tkác I, Rao R, Georgieff MK, Gruetter R. Developmental and regional changes in the neurochemical profile of the rat brain determined by *in vivo* ^{1}H NMR spectroscopy. Magn Reson Med. 2003; 50:24–32. [PubMed: 12815675]

60. Toga AW, Thompson PM. Mapping brain asymmetry. Nat Rev Neurosci. 2003; 4:37–48. [PubMed: 12511860]
61. Diamond MC, Murphy GM Jr, Akiyama K, Johnson RE. Morphologic hippocampal asymmetry in male and female rats. Exp Neurol. 1982; 76:553–565. [PubMed: 7084374]
62. Diamond MC, Johnson RE, Young D, Singh SS. Age-related morphologic differences in the rat cerebral cortex and hippocampus: Male-female; right-left. Exp Neurol. 1983; 81:1–13. [PubMed: 6861939]
63. Moffett JR, Ross B, Arun P, Madhavarao CN, Namboodiri AM. *N*-Acetylaspartate in the CNS: from neurodiagnostics to neurobiology. Prog Neurobiol. 2007; 81:89–131. [PubMed: 17275978]
64. Halliwell B. Reactive oxygen species and the central nervous system. J Neurochem. 1992; 59:1609–1623. [PubMed: 1402908]
65. Baud O, Greene AE, Li J, Wang H, Volpe JJ, Rosenberg PA. Glutathione peroxidasecatalase cooperativity is required for resistance to hydrogen peroxide by mature rat oligodendrocytes. J Neurosci. 2004; 24:1531–1540. [PubMed: 14973232]
66. Ferriero DM. Neonatal brain injury. N Engl J Med. 2004; 351:1985–1995. [PubMed: 15525724]
67. Janáky, R.; Cruz-Aguado, R.; Oja, SS.; Shaw, CA. Glutathione in the Nervous System: Roles in Neural Function and Health and Implications for Neurological Disease. In: Lajtha, A.; Baker, G.; Dunn, S.; Holt, A., editors. Handbook of Neurochemistry and Molecular Neurobiology. New York: Springer; 2007. p. 347-399.
68. McKenna, M.; Dienel, GA.; Sonnewald, U.; Waagepetersen, H.; Schousboe, A. Energy metabolism of the brain. In: Brady, ST., et al., editors. Basic neurochemistry: principles of molecular, cellular and medical neurobiology. 8. New York: Elsevier Inc; 2012. p. 200-231.
69. Warner D, Sheng H, Batini-Haberle I. Oxidants, antioxidants and the ischemic brain. J Exp Biol. 2004; 207:3221–3231. [PubMed: 15299043]
70. Love S. Oxidative stress in brain ischemia. Brain Pathol. 1990; 9:119–131. [PubMed: 9989455]
71. Jain A, Martensson J, Stole E, Auld PAM, Meister A. Glutathione defciency lead to mitochondrial damage in brain. Proc Natl Acad Sci USA. 1991; 88:1913–1917. [PubMed: 2000395]
72. Mizui T, Kinouchi H, Chan PH. Depletion of brain glutathione by buthionine sulfoximine enhances cerebral ischemic injury in rats. Am J Physiol. 1992; 262:H313–H317. [PubMed: 1539690]
73. Eppler B, Dawson R Jr. Dietary taurine manipulations in aged male Fischer 344 rat tissue: taurine concentration, taurine biosynthesis, and oxidative markers. Biochem Pharmacol. 2001; 62:29–39. [PubMed: 11377394]
74. Lima L, Obregón F, Roussó T, Quintal M, Benzo Z, Auladell C. Content and concentration of taurine, hypotaurine, and zinc in the retina, the hippocampus, and the dentate gyrus of the rat at various postnatal d. Neurochem Res. 2004; 29:247–255. [PubMed: 14992284]
75. Kulak A, Duarte JM, Do KQ, Gruetter R. Neurochemical profile of the developing mouse cortex determined by *in vivo* ^{1}H NMR spectroscopy at 14.1 T and the effect of recurrent anaesthesia. J Neurochem. 2010; 115:1466–1477. [PubMed: 20946416]
76. Chen TS, Richie JP Jr, Lang CA. The effect of aging on glutathione and cysteine levels in different regions of the mouse brain. Proc Soc Exp Biol Med. 1989; 190:399–402. [PubMed: 2928355]
77. Stipanuk MH, Coloso RM, Garcia RAG, Banks MF. Cysteine concentration regulates cysteine metabolism to glutathione, sulfate and taurine in rat hepatocytes. J Nutr. 1992; 122:420–427. [PubMed: 1542000]
78. El Idrissi A, Trenkner E. Growth factors and taurine protect against excitotoxicity by stabilizing calcium homeostasis and energy metabolism. J Neurosci. 1999; 921:9459–9468. [PubMed: 10531449]
79. El Idrissi A, Trenkner E. Taurine regulates mitochondrial calcium homeostasis. Adv Exp Med Biol. 2003; 526:527–536. [PubMed: 12908639]
80. Chen WQ, Jin H, Nguyen M, Carr J, Lee YJ, Hu CC, Faiman MD, Schloss JV, Wu JY. Role of taurine in regulation of intracellular calcium level and neuroprotective function in cultured neurons. J Neurosci Res. 2001; 66:612–619. [PubMed: 11746381]
81. Wu H, Jin Y, Wei J, Jin H, Sha D, Wu JY. Mode of action of taurine as a neuroprotector. Brain Res. 2005; 1038:123–131. [PubMed: 15757628]

82. Chan CY, Sun H, Shah SM, Agovic MS, Friedman E, Banerjee SP. Modes of direct modulation by taurine of the glutamate NMDA receptor in rat cortex. Eur J Pharmacol. 2014; 728:167–175. [PubMed: 24485893]
83. Mujsce DJ, Christensen MA, Vannucci RC. Cerebral blood flow and edema in perinatal hypoxic-ischemic brain damage. Pediatr Res. 1990; 27:450–453. [PubMed: 2345670]
84. Risher WC, Andrew RD, Kirov SA. Real-time passive volume responses of astrocytes to acute osmotic and ischemic stress in cortical slices and *in vivo* revealed by two-photon microscopy. Glia. 2009; 57:207–221. [PubMed: 18720409]
85. Solia JM, Herranz AS, Herreras O, Lerma J, Del Rio RM. Does taurine act as an osmoregulatory substance in the rat brain. Neurosci Lett. 1988; 91:53–58. [PubMed: 3173785]
86. Wade JV, Olson JP, Samson FE, Nelson SR, Pazdernik TL. A possible role for taurine in osmoregulation within the brain. J Neurochem. 1988; 51:740–745. [PubMed: 3411323]
87. Schaffer S, Takahashi K, Azuma J. Role of osmoregulation in the actions of taurine. Amino Acid. 2000; 19:527–546.
88. Thurston JH, Sherman WR, Hauhart RE, Kloepper RF. *myo*-inositol: a newly identified nonnitrogenous osmoregulatory molecule in mammalian brain. Pediatr Res. 1989; 26:482–485. [PubMed: 2812900]
89. Vitvitsky V, Garg SK, Banerjee R. Taurine biosynthesis by neurons and astrocytes. J Biol Chem. 2011; 37:32002–32110. [PubMed: 21778230]
90. Rae CD. A guide to the metabolic pathways and function of metabolites observed in human brain ^{1}H magnetic resonance spectra. Neurochem Res. 2014; 39:1–36. [PubMed: 24258018]
91. Davies SE, Gotoh M, Richard DA, Obrenovitch TP. 1998 Hypoosmolarity induces an increase of extracellular Nacetylaspartate concentration in the rat striatum. Neurochem Res. 1998; 23:1021–1025. [PubMed: 9704590]
92. Lohr JW, McReynold J, Grimaldi T, Acara M. Effect of acute and chronic hypernatremia on myo-inositol and sorbitol concentration in rat brain and kidney. Life Sci. 1988; 43:271–276. [PubMed: 3398699]
93. Dombrowski GJ Jr, Swiatek KR, Chao KL. Lactate, 3-hydroxybutyrate, and glucose as substrates for the early postnatal rat brain. Neurochem Res. 1989; 14:667–475. [PubMed: 2779727]
94. Pellerin L, Pellegri G, Martin JL, Magistretti PJ. Expression of monocarboxylate transporter mRNAs in mouse brain: Support for a distinct role of lactate as an energy substrate for the neonatal vs adult brain. Proc Natl Acad Sci USA. 1998; 95:3990–3995. [PubMed: 9520480]
95. Wallimann T, Tokarska-Schlattner M, Schlattner U. The creatine kinase system and pleiotropic effects of creatine. Amino Acid. 2001; 40:1271–1296.
96. Urenjak J, Williams SR, Gadian DG, Noble M. Proton nuclear magnetic resonance spectroscopy unambiguously identifies different neuralcell types. J Neurosci. 1993; 13:981–989. [PubMed: 8441018]
97. Kreis R, Ernst T, Ross BD. Development of the human brain: *In vivo* quantification of metabolite and water content with proton magnetic resonance spectroscopy. Magn Reson Med. 1993; 30:424–437. [PubMed: 8255190]
98. Ireland Z, Russell AP, Wallimann T, Walker DW, Snow R. Developmental changes in the expression of creatine synthesizing enzymes and creatine transporter in a precocial rodent, the spiny mouse. BMC Dev Biol. 200910.1186/1471-213X-9-39
99. Fiskum, G.; Liu, Y.; Bogaert, YE.; Rosenthal, RE.; Krieglstein, J.; Oberpichler-Schwenk, H. Acetyl-l-carnitine stimulates cerebral oxidative metabolism and inhibits protein oxidation following cardiac arrest in dogs. In: Krieglstein, J., editor. Pharmacology of cerebral ischemia. Wissenschaftliche Verlagsgesellschaft mbH; Stuttgart: 1992. p. 487-491.
100. Calabrese V, Ravagna A, Colombrita C, Scapagnini G, Guagliano E, Calvani M, Butterfield DA, Guiffrida Stella AM. Acetylcarnitine induces heme oxygenase in rat astrocytes and protects against oxidative stress: involvement of the transcription factor Nrf2. J Neurosci Res. 2005; 79:509–521. [PubMed: 15641110]
101. Rosenthal RE, Williams R, Bogaert YE, Getson PR, Fiskum G. Prevention of postischemic canine neurological injury through potentiation of brain energy metabolism by acetyl-L-carnitine. Stroke. 1992; 23:1312–1317. [PubMed: 1519288]

102. Winter BK, Fiskum G, Gallo LL. Effects of L-carnitine on serum triglyceride and cytokine levels in rat models of cachexia and septic shock. Br J Cancer. 1995; 72:1173–1179. [PubMed: 7577464]

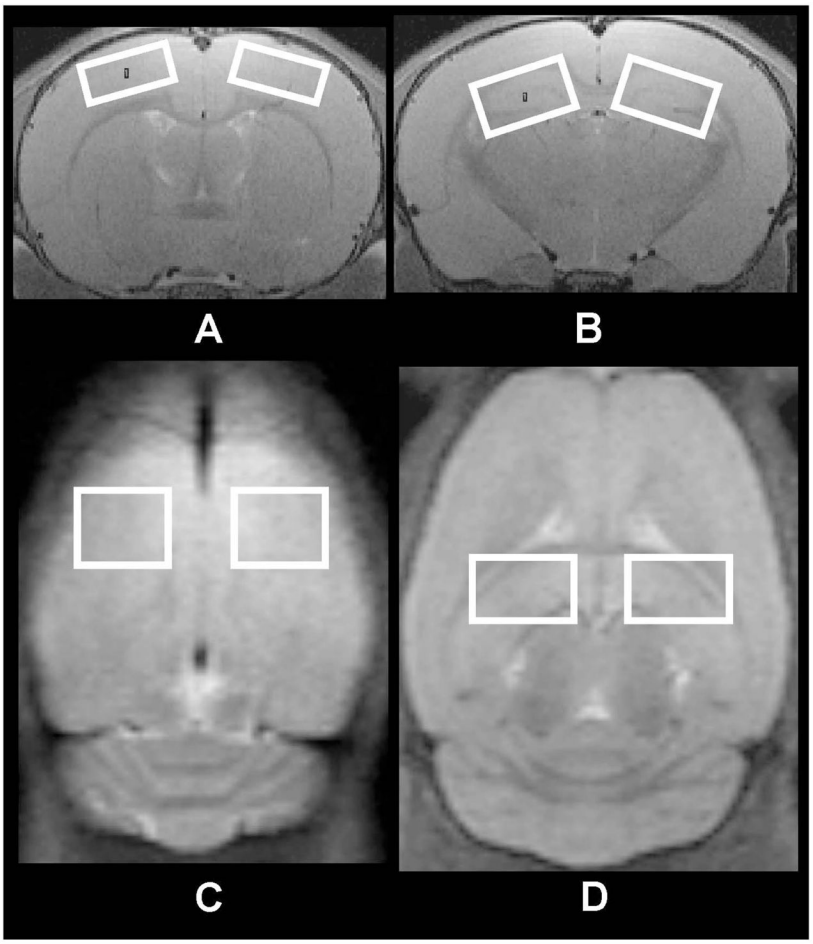

Fig. 1.

Voxel location and sizes for the *in vivo* high resolution proton MRS in a rat brain. (a) Left (contralateral) and right (ipsilateral) cortex in the coronal view of the rat brain (3.5 × 1.5 mm^2; (b) Left (contralateral) and right (ipsilateral) hippocampus in the coronal view of the rat brain (3.5 × 2.0 mm^2); (c) Left and right cortex in the axial view of the rat brain (3.5 × 3.0 mm^2); (d) Left and right hippocampus in the axial view of the rat brain (3.5 × 2.5 mm^2).

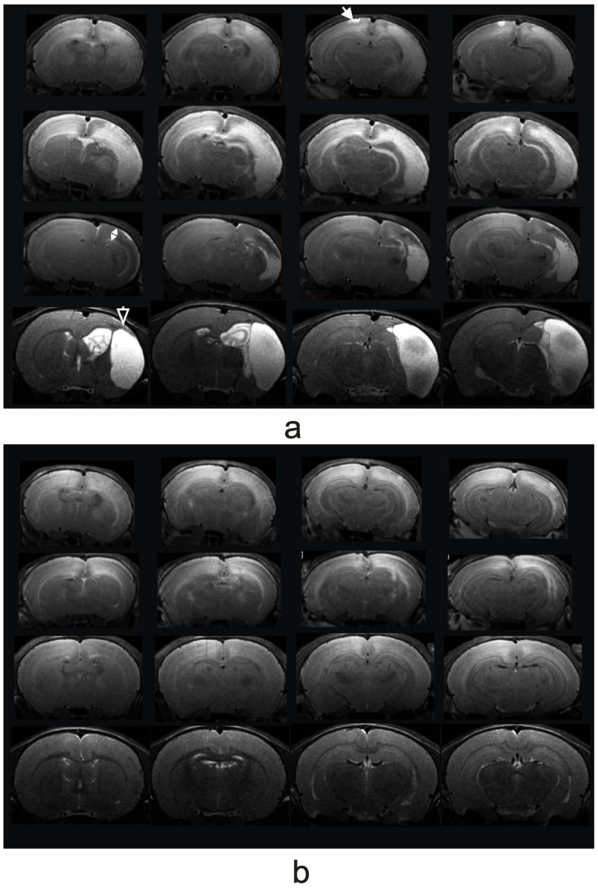

Fig. 2.

T_2-weighted MRI coronal views from a male HI (a) and a male HI+ALCAR (b) rat on 24 h (top row), 72 h (second row), 7 d (third row), and 28 d (bottom row) post HI injury. The white closed arrow shows a lesion extended to the surface of the contralateral cortex in the HI rat. The white two-head arrow indicates a cortical thinning. The white open arrow shows a cyst with discrete boundaries in the HI rat.

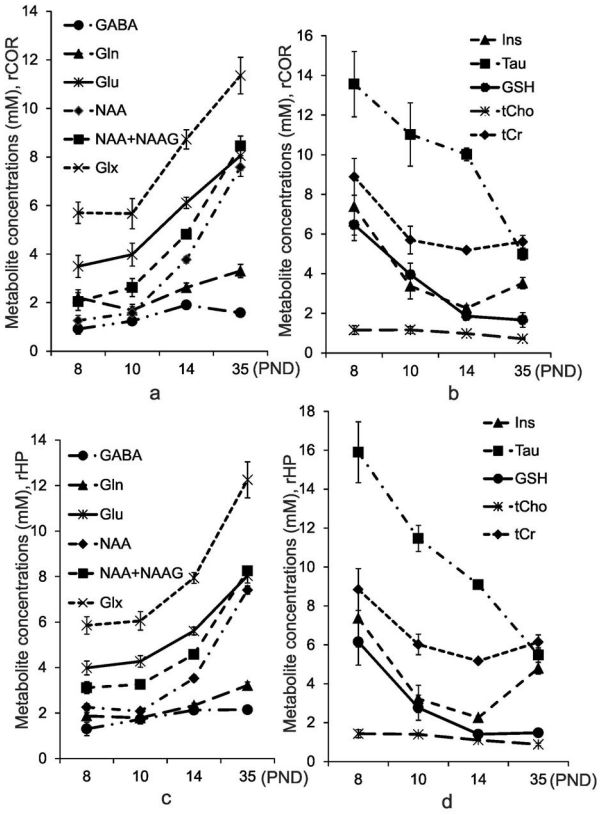

Fig. 3.

Metabolic changes during growth in the control group of the rat pups (mean ± SE, n=12). (a) and (b) The ipsilateral cortex; (c) and (d) The ipsilateral hippocampus.

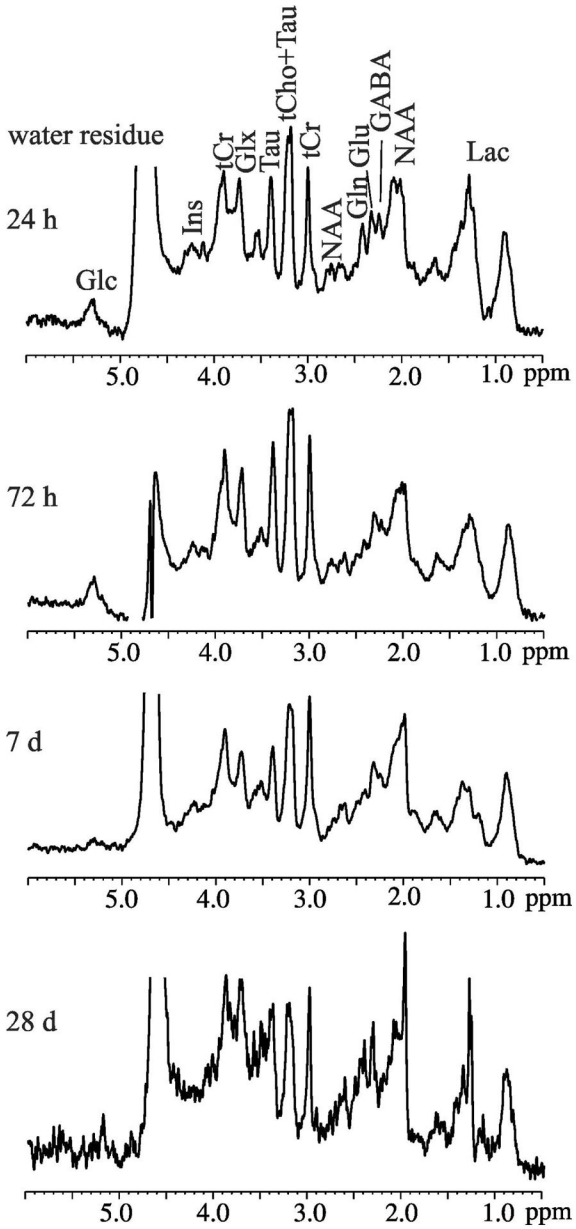

Fig. 4.

In vivo proton MRS acquired in the ipsilateral hippocampus of a male HI rat (MRI changes shown in Fig. 2a) at 24 h, 72 h, 7 d, and 28 d post injury. All the spectra were scaled to the tCr concentrations measured by LCModel ([tCr]= 4.3 mM (24 h), 6.7 mM (72 h), 4.8 mM (7 d), 6.2 mM (28 d). g-aminobutyric acid (GABA), glucose (Glc), glutamine (Gln), glutamate (Glu), glutathione (GSH), *myo*-inositol (Ins), lactate (Lac), *N*-acetylaspartate (NAA), taurine (Tau), total creatine (tCr), total choline (tCho), and glutamate/glutamine complex (Glx). All the spectra were scaled to the tCr concentrations.

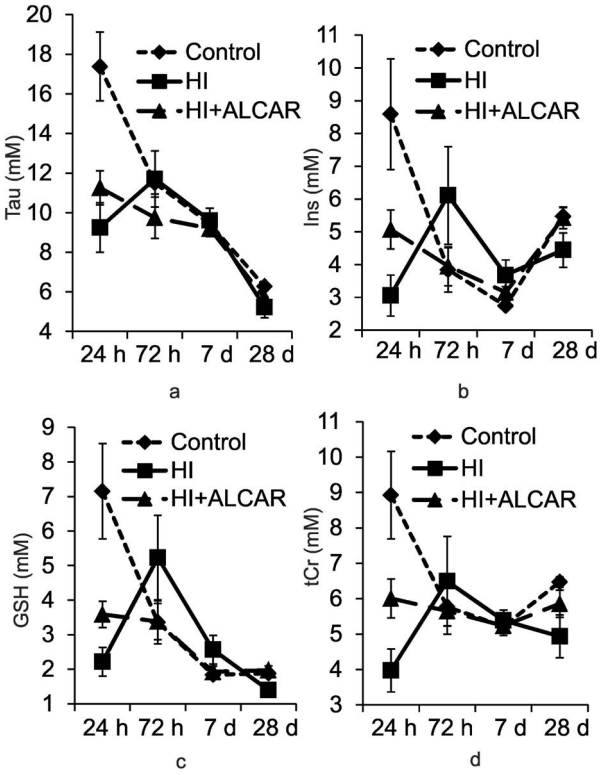

Fig. 5.

Comparisons of the concentrations (mean ± SE mM) of Tau, Ins, GSH, and tCr among the three groups of rats (Control, HI, and HI+ALCAR, n=12 in each group) in the ipsilateral hippocampus at different time points. (a) Tau; (b) Ins; (c) GSH; (d) tCr. taurine (Tau), *myo*-inositol (Ins), glutathione (GSH), and total creatine (tCr).

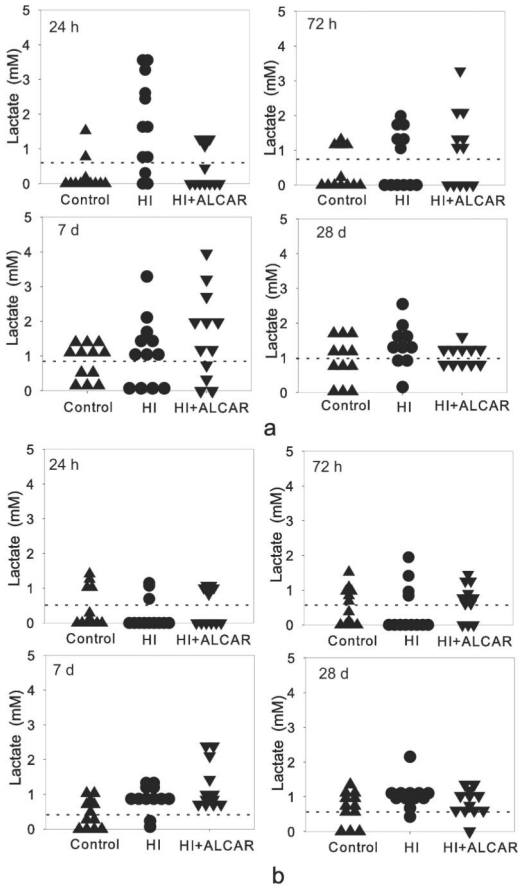

Fig. 6.

Lactate distribution maps (individual mark represents a single animal) (a) ipsilateral hippocampus; (b) contralateral hippocampus.

Table 1

Concentrations of metabolites in the hippocampus of the immature rat brains.

	24 hours			72 hours			7 days			28 days		
	Control	**HI**	**HI+ALCAR**	**Control**	**HI**	**HI+ALCAR**	**Control**	**HI**	**HI+ALCAR**	**Control**	**HI**	**HI+ALCAR**
ipsilateral hippocampus												
GABA	1.30±0.29	1.39±0.13	1.29±0.22	1.72±0.19	0.98±0.19	1.24±0.20	2.13±0.07	1.64±0.21	1.97±0.16	2.02±0.19	1.72±0.25	2.06±0.20
Gln	1.87±0.14	2.16±0.26	2.19±0.19	1.78±0.17	1.41±0.21	1.81±0.19	2.33±0.11	2.39±0.27	2.63±0.15	3.06±0.23	2.77±0.25	2.99±0.22
Glu	3.98±0.31	3.58±0.40	3.33±0.46	4.27±0.25	2.86±0.39	3.39±0.47	5.61±0.17	4.77±0.53	5.65±0.43	7.37±0.62	6.38±0.73	6.76±0.60
Ins	8.09±1.69	2.56±0.62	4.57±0.60	3.34±0.68	5.61±1.49	3.45±0.59	2.24±0.09	3.18±0.46	2.65±0.17	4.65±0.34	3.94±0.53	4.93±0.33
NAA	2.25±0.15	1.50±0.19	1.51±0.25	2.08±0.13	1.99±0.20	1.68±0.30	3.52±0.13	3.40±0.27	3.70±0.27	6.79±0.64	5.81±0.68	6.34±0.65
Tau	16.88±1.73	8.75±1.25	10.76±0.86	11.00±0.56	11.20±1.42	9.24±1.05	8.95±0.20	9.11±0.61	8.70±0.41	5.40±0.37	4.72±0.53	5.18±0.38
GSH	6.65±1.38	1.72±0.42	3.09±0.38	2.86±0.62	4.73±1.22	2.88±0.52	1.34±0.11	2.07±0.42	1.42±0.17	1.48±0.11	0.90±0.18	1.47±0.13
tCho	1.30±0.19	1.23±0.12	1.43±0.12	1.32±0.08	1.12±0.09	1.32±0.09	1.12±0.03	1.06±0.07	1.18±0.05	0.86±0.07	0.86±0.10	0.96±0.07
NAA+NAAG	3.12±0.26	2.18±0.32	2.45±0.40	3.25±0.12	2.47±0.26	2.46±0.43	4.58±0.14	4.41±0.31	4.70±0.34	7.63±0.66	6.42±0.75	7.24±0.67
tCr	8.93±1.23	3.97±0.61	6.01±0.55	5.77±0.53	6.49±1.26	5.65±0.64	5.21±0.12	5.38±0.30	3.83±0.41	6.05±0.38	4.93±0.61	5.85±0.38
Glx	5.85±0.38	5.74±0.57	5.52±0.40	6.05±0.40	4.27±0.46	5.20±0.55	7.94±0.24	7.16±0.69	5.67±0.53	10.43±0.79	9.15±0.95	9.75±0.77
contralateral hippocampus												
GABA	1.17±0.15	1.08±0.22	1.17±0.21	1.54±0.09	1.55±0.18	1.68±0.09	2.01±0.11	1.89±0.05	1.83±0.13	2.21±0.09	2.19±0.07	1.73±0.14
Gln	1.82±0.24	1.51±0.18	1.70±0.18	1.55±0.14	1.45±0.15	1.55±0.10	2.10±0.13	2.24±0.21	2.23±0.24	2.88±0.18	3.00±0.12	2.96±0.12
Glu	3.36±0.37	3.59±0.30	3.40±0.39	4.04±0.15	4.16±0.20	4.12±0.13	5.21±0.16	5.33±0.24	5.42±0.32	7.54±0.26	7.74±0.19	7.38±0.24
Ins	6.16±1.34	5.96±1.54	6.56±1.65	2.69±0.35	4.44±0.73	3.46±40	2.94±0.24	2.31±0.23	2.72±0.20	4.94±0.19	5.06±0.24	5.18±0.16
NAA	1.47±0.21	1.35±0.21	1.58±0.16	1.76±0.08	2.06±0.12	2.00±0.07	3.18±0.07	3.46±0.13	3.50±0.12	6.54±0.14	6.52±0.10	6.57±0.16
Tau	12.75±2.05	14.03±1.49	13.21±1.72	10.39±0.35	13.83±0.84	11.22±0.47	8.87±0.24	9.26±0.26	9.15±0.27	5.66±0.11	5.71±0.09	5.55±0.11
GSH	5.31±1.04	4.88±1.30	5.43±1.31	2.59±0.40	4.30±0.70	3.04±0.32	1.68±0.24	1.70±0.22	1.82±0.32	1.45±0.10	1.53±0.07	1.44±0.06
tCho	1.48±0.18	1.14±0.16	1.38±0.17	1.33±0.03	1.53±0.14	1.55±0.06	1.16±0.03	1.14±0.03	1.17±0.04	1.01±0.04	1.05±0.02	0.98±0.03
NAA+NAAG	2.17±0.26	2.37±0.22	2.26±0.27	2.86±0.16	3.47±0.19	3.06±0.09	4.18±0.12	4.54±0.13	4.49±0.17	7.38±0.15	7.35±0.12	7.39±0.15
tCr	7.79±1.08	6.96±1.05	7.88±1.16	4.93±0.23	6.70±0.52	5.45±0.27	5.14±0.09	5.26±0.10	5.24±0.11	6.07±0.14	6.23±0.09	6.18±0.12
Glx	5.18±0.36	5.10±0.45	5.10±0.46	5.59±0.25	5.61±0.28	5.66±0.21	7.31±0.27	7.57±0.32	7.65±0.53	10.43±0.33	10.74±0.22	10.34±0.28

Values are mean ± standard error mM

Table 2

Concentrations of metabolites in the cortex of the immature rat brains

	24 hours			72 hours			7 days			28 days		
	Control	**HI**	**HI+ALCAR**	**Control**	**HI**	**HI+ALCAR**	**Control**	**HI**	**HI+ALCAR**	**Control**	**HI**	**HI+ALCAR**
ipsilateral cortex												
GABA	1.08±0.19	0.90±0.29	0.99±0.27	1.29±0.21	0.73±0.15	1.19±0.23	2.01±0.11	1.40±0.17	1.56±0.17	1.74±0.17	1.93±0.11	1.73±0.14
Gln	1.99±0.37	2.13±0.24	2.06±0.23	1.73±0.23	1.33±0.16	1.92±0.32	2.56±0.20	2.31±0.36	2.87±0.19	3.33±0.27	3.21±0.20	3.28±0.30
Glu	3.74±0.35	3.23±0.57	3.52±0.65	3.83±0.50	2.57±0.49	3.94±0.42	6.07±0.23	5.44±0.49	5.65±0.47	8.06±0.59	8.48±0.61	8.29±0.46
Ins	7.53±1.38	5.19±1.16	5.66±1.02	4.26±1.21	2.55±0.62	3.14±0.96	2.24±0.16	2.84±0.33	2.54±0.25	3.47±0.30	3.61±0.27	3.59±0.26
NAA	1.61±0.18	0.88±0.19	1.07±0.21	1.51±0.23	0.98±0.30	1.68±0.25	3.46±0.28	3.52±0.28	3.33±0.41	7.47±0.40	7.45±0.45	7.62±0.37
Tau	15.13±1.44	10.77±2.01	12.99±2.00	11.42±1.70	6.70±1.50	11.03±1.43	10.78±0.75	10.02±0.73	9.35±0.71	4.98±0.29	4.78±0.25	4.58±0.27
GSH	6.40±0.86	3.92±0.77	4.93±0.55	4.57±0.94	2.81±0.74	2.76±0.59	2.21±0.37	2.09±0.44	1.89±0.28	1.71±0.39	1.32±0.20	1.44±0.17
tCho	1.09±0.19	1.14±0.18	1.27±0.20	1.07±0.18	0.92±0.15	1.08±0.15	0.99±0.04	0.98±0.04	1.01±0.09	0.72±0.04	0.79±0.04	0.79±0.04
NAA+NAAG	2.47±0.28	1.46±0.39	1.88±0.42	2.41±0.34	1.45±0.44	2.63±0.40	4.61±0.23	4.38±0.35	4.28±0.47	8.35±0.41	8.22±0.52	8.54±0.40
tCr	7.98±0.99	7.26±1.03	7.58±0.83	6.25±0.94	4.04±0.88	5.02±0.86	5.27±0.20	5.10±0.34	4.91±0.35	5.58±0.32	5.32±0.40	5.46±0.32
Glx	5.73±0.42	5.36±0.67	5.58±0.73	5.56±0.64	3.91±0.56	5.86±0.65	8.64±0.41	7.75±1.63	8.51±0.62	11.40±0.74	11.69±0.75	11.57±0.69
contralateral cortex												
GABA	0.93±0.19	1.28±0.23	0.91±0.24	1.39±0.17	1.26±0.09	1.54±0.13	1.94±0.13	1.71±0.06	1.75±0.06	1.96±0.14	1.88±0.09	1.80±0.10
Gln	1.84±0.17	1.71±0.23	2.36±0.21	1.66±0.19	1.38±0.13	1.57±0.16	2.06±0.16	2.37±0.17	2.46±0.22	3.07±0.16	2.91±0.10	2.98±0.20
Glu	3.60±0.44	3.93±0.51	3.61±0.55	3.86±0.47	4.04±0.28	4.64±0.26	5.58±0.25	5.84±0.27	6.06±0.16	8.35±0.31	9.08±0.28	8.37±0.25
Ins	6.07±1.70	4.40±0.83	6.82±1.25	2.42±0.47	2.09±0.29	2.28±0.17	2.20±0.19	2.38±0.17	2.13±0.21	3.58±0.18	3.77±0.22	3.83±0.21
NAA	1.24±0.21	0.98±0.16	0.82±0.17	1.67±0.27	1.79±0.13	1.92±0.08	2.99±0.36	3.88±0.15	3.71±0.09	7.65±0.23	8.07±0.17	7.88±0.13
Tau	13.69±1.89	13.69±1.81	13.85±2.20	9.60±1.48	11.23±0.86	12.99±0.91	11.70±1.30	10.12±0.21	10.05±0.16	5.14±0.11	4.99±0.12	5.01±0.15
GSH	6.00±1.23	5.04±0.41	6.63±0.88	3.41±0.48	3.34±0.28	3.56±0.19	2.94±0.33	2.18±0.22	1.97±0.29	1.73±0.13	1.67±0.11	1.97±0.31
tCho	1.12±0.15	1.39±0.18	1.33±0.15	1.13±0.15	1.08±0.09	1.34±0.08	1.14±0.14	0.97±0.03	0.99±0.03	0.76±0.03	0.81±0.03	0.79±0.02
NAA+NAAG	1.96±0.33	2.12±0.32	1.57±0.32	2.60±0.38	2.97±0.22	3.17±0.11	4.16±0.28	4.86±0.16	4.71±0.08	8.56±0.22	8.93±0.16	8.76±0.10
tCr	8.08±1.08	7.24±0.59	8.95±0.97	5.15±0.66	4.86±0.37	5.32±0.29	5.41±0.38	5.08±0.09	5.04±0.07	5.69±0.13	5.88±0.13	5.81±0.07
Glx	5.45±0.34	5.64±0.55	5.97±0.57	5.51±0.61	5.42±0.38	6.21±0.41	7.64±0.38	8.21±0.28	8.52±0.36	11.41±0.38	11.99±0.29	11.35±0.39

Values are mean ± standard error (mM).

Table 3

Two-way repeated measures ANOVA for each metabolite in the hippocampus.

	Time				Group * Time			
	Ipsilateral		Contralateral		Ipsilateral		Contralateral	
	F (3,97)	P	F (3,97)	P	F (6,97)	P	F (6,97)	P
GABA	13.330	**<0.001**	32.537	**<0.001**	1.710	0.127	0.286	0.942
Gln	20.611	**<0.001**	39.923	**<0.001**	0.835	0.546	0.358	0.903
Glu	50.612	**<0.001**	134.656	**<0.001**	0.636	0.702	0.164	0.986
Glx	46.474	**<0.001**	141.387	**<0.001**	0.844	0.539	0.174	0.983
GSH	11.941	**<0.001**	19.571	**<0.001**	5.730	**<0.001**	0.613	0.719
Ins	5.228	**0.002**	12.023	**<0.001**	5.174	**<0.001**	0.507	0.802
NAA	134.134	**<0.001**	762.543	**<0.001**	0.819	0.558	0.623	0.712
NAA+NAAG	115.354	**<0.001**	412.427	**<0.001**	0.744	0.615	0.582	0.744
Tau	35.751	**<0.001**	40.139	**<0.001**	6.358	**<0.001**	0.826	0.552
tCho	12.362	**<0.001**	14.430	**<0.001**	0.271	0.949	1.902	0.088
tCr	1.510	0.217	5.614	**<0.001**	4.206	**<0.001**	1.320	0.256

Groups include Control, HI, and HI+ALCAR rats. Time points include 24 hours, 72 hours, 7 days, and 28 days post injury.

Table 4

Two-way repeated measures ANOVA for each metabolite in the cortex.

	Time				Group * Time			
	Ipsilateral		Contralateral		Ipsilateral		Contralateral	
	F (3,97)	P	F (3,97)	P	F (6,97)	P	F (6,97)	P
GABA	16.420	**<0.001**	25.090	**<0.001**	1.425	0.213	1.687	0.132
Gln	24.316	**<0.001**	33.007	**<0.001**	0.518	0.793	1.158	0.335
Glu	76.033	**<0.001**	141.399	**<0.001**	0.813	0.562	0.836	0.545
Glx	77.065	**<0.001**	146.173	**<0.001**	0.765	0.599	0.699	0.651
GSH	25.490	**<0.001**	39.857	**<0.001**	1.22	0.300	0.851	0.534
Ins	14.265	**<0.001**	20.037	**<0.001**	1.228	0.298	1.173	0.327
NAA	406.211	**<0.001**	842.716	**<0.001**	1.080	0.380	1.965	0.078
NAA+NAAG	252.238	**<0.001**	620.535	**<0.001**	0.941	0.469	1.314	0.258
Tau	23.307	**<0.001**	30.671	**<0.001**	1.256	0.285	0.878	0.514
tCho	3.987	**0.01**	11.572	**<0.001**	0.545	0.773	1.137	0.347
tCr	12.255	**<0.001**	23.004	**<0.001**	0.632	0.704	0.727	0.629

Groups include Control, HI, and HI+ALCAR rats. Time points include 24 hours, 72 hours, 7 days, and 28 days post injury.